

Stability Analysis of Rock Slopes with Stochastic Fractures using Finite Element Limit Analysis

A.M. Lester¹, A.V. Lyamin¹, N.C. Podlich¹, J. Huang¹ and A. Giacomini¹

¹Priority Research Centre for Geotechnical Science and Engineering, The University of Newcastle, Callaghan NSW 2308, Australia.

E-mail: alexander.lester@uon.edu.au, andrei.lyamin@newcastle.edu.au, nathan.podlich@newcastle.edu.au, jinsong.huang@newcastle.edu.au, anna.giacomini@newcastle.edu.au.

Abstract: Rock slopes are commonly encountered in geotechnical engineering practice, and yet there is significant uncertainty when it comes to assessment of their stability, on account of the unknown extent of fracturing within the slope. Even where detailed mapping of fractures has been carried out on exposed rock faces, the unmapped extent of fracturing within the slope can still significantly affect its stability. This has previously motivated stochastic modelling of fractures, with Monte Carlo simulations carried out based on different, randomly generated discrete fracture networks (DFNs) to estimate a probability of failure for the slope. Until recently, displacement-based numerical methods such as the finite element method (FEM) have been used to perform such simulations under general loading conditions. However, convergence upon a strength reduction factor defining the onset of failure is not guaranteed when using FEM, and a much more efficient and reliable method of stability analysis under general loading conditions is finite element limit analysis (FELA). In this study, FELA is applied in probabilistic strength reduction analysis of two fractured rock slopes, with DFNs generated using a new algorithm that takes account of positions and orientations of fractures observed on exposed faces of the rock. Analysis of the second slope is also attempted using a commercial FEM package, and the advantages of adopting FELA over this approach are clearly demonstrated.

Keywords: Rock slopes; limit analysis; strength reduction analysis; discrete fracture networks; probabilistic slope stability analysis.

1 Introduction

Rock slope instability poses a significant threat to people and property on account of the risk of sudden collapse, and is an issue which frequently presents itself during the course of civil engineering projects. There is a tendency for the risk of collapse to be dangerously underestimated, particularly when comprehensive knowledge of a rock mass's structure and the arrangement of its fractures cannot be fully obtained by surface mapping only. The inability to pick up hidden fractures during field investigation constitutes a major source of uncertainty when it comes to stability assessment of rock slopes.

There are a number of approaches which have previously been employed when it comes to analysis of rock slope stability, and the oldest and simplest of these is limit equilibrium, which is still widely used by practitioners to gain a first approximation for the factor of safety (FoS) defining failure. A good summary of various limit equilibrium approaches for rock slopes has been given by Hoek and Bray (1981). However, a significant drawback of limit equilibrium is that a failure mechanism needs to be assumed prior to analysis, and this mechanism is often highly dependent on the geometry of hidden fractures that can't be picked up via mapping of exposed rock faces only.

An approach where the geometry of fractures can be modelled explicitly, without necessarily being known at the outset, is stochastic modelling of fractures. In this approach, geometric parameters such as position, orientation and persistence (fracture extension within the rock mass) are chosen randomly from specified probability distributions of sets of structures observed during field investigation. Monte Carlo simulations can then be performed based on different, randomly generated discrete fracture networks (DFNs), and from this the probability of failure for a rock slope can be estimated. The Monte Carlo simulations can be combined with a numerical modelling approach such as the finite element method (FEM), where calculation of displacements via the application of load steps allows failure mechanisms to be discerned without them having to be assumed prior to analysis. Most commercial FEM programs also include a routine to perform strength reduction analysis, where the values of the strength parameters required to initiate collapse are determined via an iterative process (e.g. Brinkgreve and Bakker 1991; Hammah et al. 2004; Dyson and Tolooiyan 2018). The factor by which the strength parameters are reduced in order to cause failure is termed the strength reduction factor (SRF), and when using the Mohr-Coulomb failure criterion, the SRF is usually defined such that it is equal to the FoS.

Despite its usefulness in conducting analysis under general loading conditions, strength reduction analysis via FEM can be computationally expensive, particularly when many Monte Carlo simulations are being performed. Additionally, convergence upon a value for the SRF is not guaranteed, and any converged SRF is likely to be erroneous due to the inability of FEM to model post-failure behaviour. A much faster and more robust method of

stability analysis under general loading conditions is finite element limit analysis (FELA). Originally, FELA was developed as a method for determining tight upper and lower bounds on the collapse multiplier of a geostructure (Sloan 2013). The collapse multiplier is defined as the fraction of the applied load or material unit weight required to initiate collapse, and is different to the SRF which is a multiplier on the material strength parameters. However, by using a different formulation of the optimisation problems solved in FELA, it is possible to obtain the SRF as the output rather than the collapse multiplier (Krabbenhøft and Lyamin 2015). This is more meaningful when comparing results with other methods of stability analysis, particularly in light of the equivalence between the SRF and FoS when using the Mohr-Coulomb criterion.

In this study, the method of strength reduction FELA as developed by Krabbenhøft and Lyamin (2015) is applied in probabilistic stability analysis of two fractured rock slopes modelled using the Mohr-Coulomb failure criterion. Analysis of the second slope is also attempted using the commercial FEM package RS2, developed by Rocscience. DFNs analysed via FELA are generated using a new algorithm which takes account of the position and orientation of fractures observed during field investigation. To the authors' knowledge, this is the first time that FELA has been combined with stochastic modelling of fractures as a means of assessing rock slope stability. In Section 2, a description of the new fracture generation algorithm is provided, and details of the example problems together with results and discussion are then given in Section 3.

2 Fracture Generation Algorithm

The fracture generation algorithm introduced in this study is based on an algorithm for generating conditional DFNs in two dimensions originally devised by Andersson et al. (1984). 'Conditional' means that fractures are generated according to information that is known about fractures observed within the rock mass during field investigation. Andersson et al. (1984) started by considering a fracture of infinite length, defined by a radius (r) and orientation (ψ) relative to a fixed origin, and then introduced the additional parameters of length (L) and centre point location (s) for extension to fractures of finite length. In this study, the parameters defining fractures of finite length are adopted, and are depicted in Figure 1 using an example outline of a rock mass. The value of s is defined as the distance between the midpoint of the fracture, and the midpoint of the two furthest points at which the fracture line intersects the outline of the rock mass.

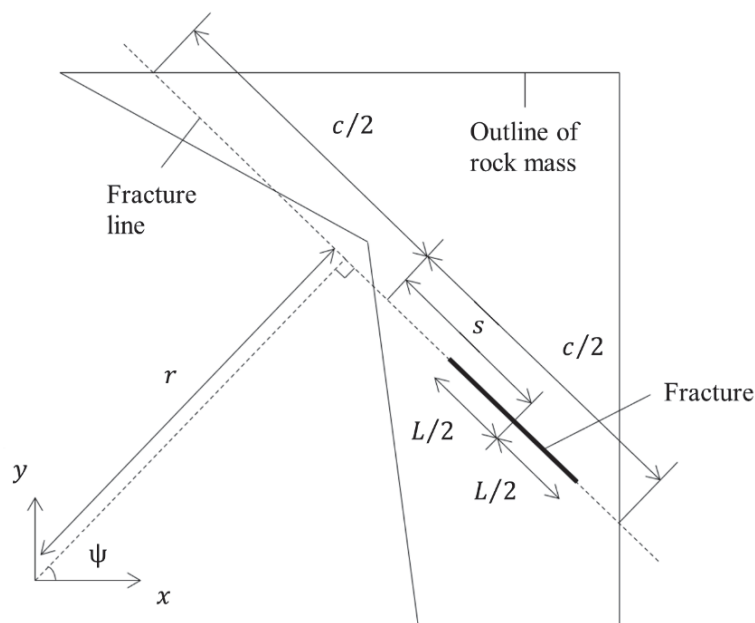


Figure 1. Definition for fractures of finite length according to Andersson et al. (1984)

Readers are referred to Andersson et al. (1984) for details of the fracture generation algorithm that they developed. In brief, the algorithm accounts for fractures which have been observed in boreholes drilled into the rock mass (referred to here as known fractures), and seeks to determine the probability that any fracture located within the rock mass will intersect at least one of the boreholes. A negative binomial distribution is then employed to generate a number of additional fractures that do not intersect any boreholes, and the geometric parameters of these fractures (r , ψ , L and s) are chosen randomly from uniform distributions. In this study, a number of extensions are made to the algorithm of Andersson et al. (1984) which facilitate its application to practical problems, and these extensions are outlined as follows:

1. Problem domain – Andersson et al. (1984) considered a circle as a representative domain in which fractures can be generated for 2D problems. The larger the circle is, the less that the DFN generated within the

rock mass will be influenced by boundary effects. However, there are already other measures within the algorithm aimed at mitigating boundary effects, and so for simplicity the algorithm adopted in this study considers the modelled rock mass itself to be the representative domain in which fractures are generated. The outline of the rock mass can be any polygon defined as a series of points connected by straight lines.

2. Maximum fracture radius and length – The maximum radius to a fracture (r_{max}) is here defined as the maximum distance from the origin to any of the points defining the outline of the rock mass. For simplicity, the maximum fracture length (L_{max}) is chosen as the greatest distance between any two points defining the outline of the rock mass. The fracture length, however, is not constrained to lie entirely within the rock mass, which minimises bias in the layout of DFNs with respect to the rock mass outline.

3. Generalisation of ‘boreholes’ to ‘observation surfaces’ – Andersson et al. (1984) only accounted for known fractures which had been observed in boreholes. However, fractures can be observed by other means, such as at the ground surface or inside a tunnel. In this study, the term ‘observation surface’ is introduced to describe any segment of the rock mass outline on which known fractures may be defined and included as part of the DFNs generated by the fracture generation algorithm.

4. Definition of known fractures – In this study, the position and orientation of known fractures, which define the values of r and ψ , are assumed known and accepted as user input. The values of the remaining parameters L and s are assumed unknown and are randomly generated.

5. Generating lengths for known fractures – Given that there is a higher probability of observing a longer fracture than a shorter one, it is inappropriate to generate lengths for known fractures based on a uniform distribution, something which was recognised by Andersson et al. (1984). In the algorithm introduced in this study, a series of individual random fractures are generated prior to performing the Monte Carlo simulations of DFNs, and the lengths of fractures which intersect observation surfaces are saved in memory. Length values for known fractures generated as part of the Monte Carlo simulations are then selected from these saved lengths.

A summary of the steps followed by the fracture generation algorithm is provided below:

1. Calculate r_{max} and L_{max} based on the given outline of the rock mass.
2. Generate a series of random fractures subject to r_{max} and L_{max} . Record the number of fractures (F_T) that lie partly or wholly within the slope, and the number of fractures (F_O) that intersect observation surfaces. Also save the lengths of the fractures that intersect observation surfaces for use in Step 4.
3. Estimate the probability of observing a fracture (P_O) as F_O/F_T .
4. Begin the first Monte Carlo simulation of a DFN by generating values of L and s for the known fractures. Values of L are selected from the saved lengths obtained during Step 2.
5. Generate the number of fractures additional to the known fractures that will be included in the DFN. This is done using a negative binomial distribution, with the number of known fractures and P_O as inputs.
6. Generate values of r , ψ , L and s defining the geometry of the additional fractures based on uniform distributions. If the generated parameters result in an additional fracture that intersects an observation surface, this fracture is rejected and another generated in its place.
7. Perform strength reduction FELA based on the generated DFN.
8. Repeat Steps 4-7 for each of the user specified number of Monte Carlo simulations to be carried out.

It is noted that the above algorithm generates geometric parameters for each fracture individually, with the additional fractures set at random orientations. This is at odds with how fractures are typically observed in the field, where they tend to occur in sets comprising individual fractures that are generally regularly spaced and have similar orientation. In this study, use of the fracture generation algorithm is confined to examples where known fracture sets have a wide range of orientations, such that the random orientations of additionally generated fractures are not at odds with the orientations of the known fractures.

3 Example Problems

Strength reduction FELA was carried out for two rock slopes modelled in plane strain, with the first being a 10 m high vertical slope, depicted by the solid outline in Figure 2. The second slope is inclined at 45 degrees, and represents a scenario where the first slope has been cut back to a lower inclination, indicated by the dashed outline in Figure 2. The known fractures for both slopes can be grouped into three sets, with the fracture lines oriented at $\alpha = 205^\circ$, 250° and 310° relative to the positive x axis. The wide variation in orientations makes this an appropriate test case for the fracture generation algorithm described in the previous section, where additionally generated fractures are randomly oriented. The known fractures 1-5 and 9-10 were observed at the ground surface, while fractures 6-8 were observed within a borehole drilled to a depth of 10 m.

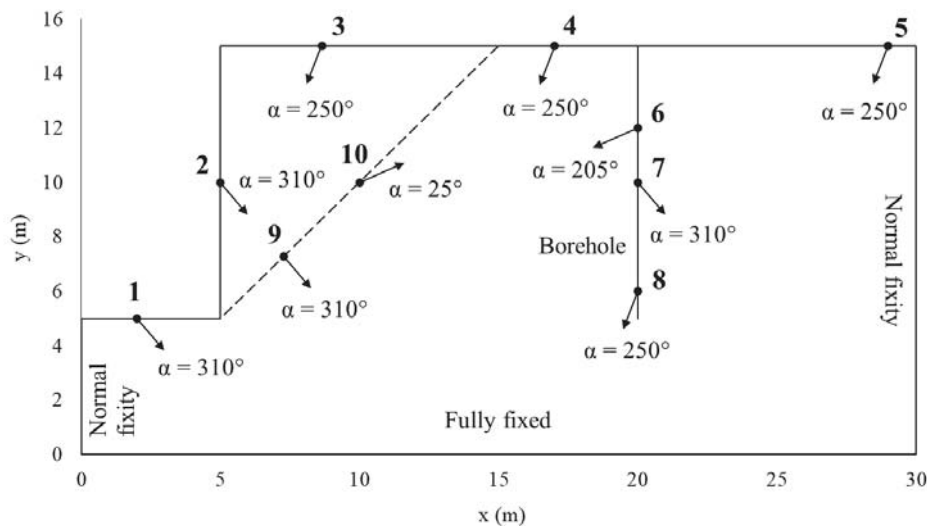


Figure 2. Outline of vertical slope (solid line) and 45 degree slope (dashed line) including known fracture positions

In the analysis of both the vertical and 45 degree slopes, restrictions were imposed upon the randomly generated lengths of the known fractures such that they did not intersect with any observation surfaces additional to the ones on which they were picked up. For example, the length of fracture 3 was restricted to less than 10.64 m such that it did not pass through the exposed toe of the slope. Fractures 1-5 and 9-10 intersecting the ground surface were made to extend at least 0.5 m into the slope. Additional fractures that did not pass through any observation surfaces were then generated as part of each Monte Carlo simulation. Both slopes were assigned a unit weight of 22 kN/m^3 , and strength parameters according to the Mohr-Coulomb criterion of $c = 50 \text{ kPa}$ and $\phi = 25^\circ$. Failure along the fractures was also defined using the Mohr-Coulomb criterion, with $c = 1 \text{ kPa}$ and $\phi = 15^\circ$. These parameters are representative of a very weak rock material which could be, for example, shale or soft limestone. Strength reduction was applied to both the intact rock material and the fractures during the strength reduction analysis.

The two slopes were modelled and analysed within Bounds, an in-house FELA program developed at the University of Newcastle, Australia. This program utilised the new fracture generation algorithm as well as the Wolf interior point solver (Podlich 2017; Wolf Optimization 2021) for the solution of conic optimisation problems. For each slope 1000 Monte Carlo simulations of different, randomly generated DFNs were performed. Within each Monte Carlo simulation, upper and lower bound estimates of the SRF were obtained via strength reduction FELA based on a uniform finite element mesh of approximately 10 000 triangular elements. Linear interpolation of stresses was used to determine the lower bound to the SRF, while quadratic interpolation of velocities was used to determine the upper bound. An overall value for the SRF was calculated for each Monte Carlo simulation as the average of the SRF values obtained from the upper and lower bound limit analyses. An additional simulation was performed without any fractures present in the slope. All analyses were performed on a Dell laptop running Windows 10, with an Intel Core i7-9850H six core CPU running at 2.6 GHz, and 64 GB of RAM.

Performing 1000 Monte Carlo simulations took approximately 11.5 hours for the vertical slope, and approximately 9.5 hours for the 45 degree slope. The probability density function (PDF) for the SRF determined from the 1000 Monte Carlo simulations is depicted in Figure 3a for the vertical slope and in Figure 3b for the 45 degree slope, with frequency plotted based on an interval of 0.1 for the SRF. The highest interval in each plot corresponds to the SRF obtained with no fractures in the slope, which was 1.26 for the vertical slope and 2.28 for the 45 degree slope. Two example DFNs for the 45 degree slope, together with their corresponding SRFs and failure mechanisms are depicted in Figure 4. The coloured contours here show relative shear dissipation, which is obtained via multiplication of the deviatoric stresses and strain rates (Lyamin et al. 2013). Red indicates a high relative magnitude of shear dissipation within the rock mass material, while blue indicates areas of low relative shear dissipation. In Figure 4a, the failure surface is clearly depicted by the bands of high shear dissipation connecting fracture 6 with the outline of the slope. In Figure 4b, fractures 4 and 10 are long enough such that they have joined up, and this leads to the block with outline shown in red to break away from the slope.

For the vertical slope, 657 of the 1000 Monte Carlo simulations returned an SRF less than 1, which gives a probability of failure (PoF) of 65.7% as shown in Figure 3a. This is relatively high, indicating that stabilisation measures are needed in order to reduce the PoF and hence the risk of failure. Higher frequencies are generally encountered for higher values of the SRF, which shows that for this particular slope, the fractures are more likely to reduce the unfractured SRF of 1.26 by a small amount (say 15%) rather than a large amount (say 70%). However, because the unfractured SRF is already relatively close to 1, introducing fractures sees the slope fail in the majority of the Monte Carlo simulations.

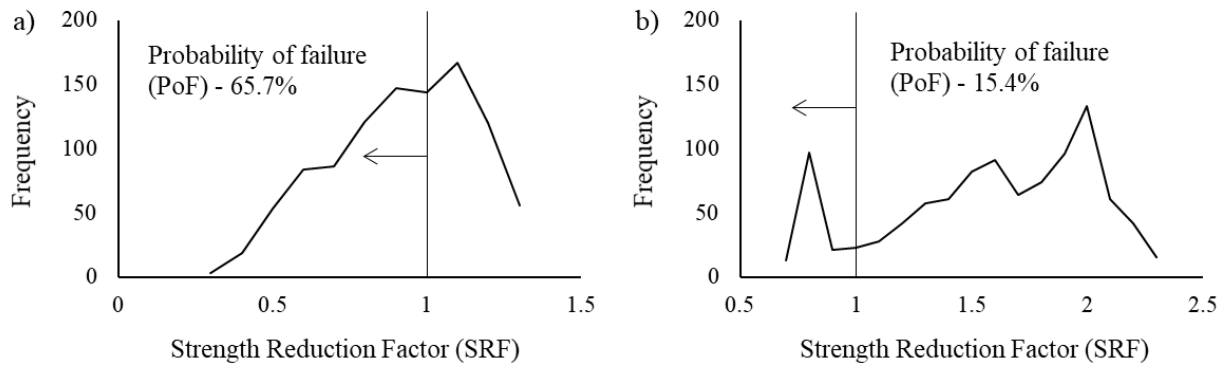


Figure 3. PDF of the SRF for a) the vertical slope and b) the 45 degree slope

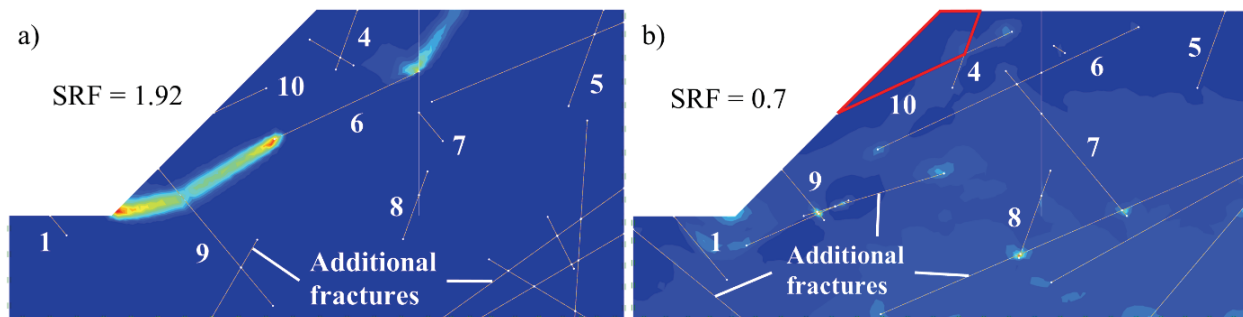


Figure 4. Plots of relative shear dissipation for two different DFNs analysed for the 45 degree slope

For the 45 degree slope the PoF is 15.4%, which is significantly lower than that for the vertical slope, and this is expected given that the slope inclination has been halved. However, the PDF for the 45 degree slope (Figure 3b) is more skewed than that of the vertical slope, with two clear peaks present. The first corresponds to the SRF interval of 1.9 - 2.0 (13.3% of simulations), while the second corresponds to the SRF interval of 0.7 - 0.8 (9.7% of simulations). Many of the simulations falling within the latter interval are ones where fracture 10 has joined up with fracture 4, leading to failure of the rock block highlighted in Figure 4b. Being able to estimate the probability of events such as this is useful when deciding what measures, if any, will be needed to stabilise the slope. Stochastic modelling of fractures in both the vertical and 45 degree slopes has effectively removed the uncertainty associated with the assumed, fixed fracture lengths that would need to be adopted when carrying out deterministic stability analysis of either slope.

Analysis of the 45 degree slope was also attempted using the commercial FEM package RS2, which has frequently been applied in stability assessment of fractured rock slopes under general loading conditions. This program allows known fractures with specific positions and orientations to be modelled, as well as additional randomly generated fractures. However, DFNs cannot be changed during the course of an analysis, meaning that Monte Carlo simulations with different DFNs have to be run manually. To start with, strength reduction analysis with RS2 was performed without any fractures, based on the 45 degree slope outline in Figure 2 and a uniform mesh of approximately 10 000 six-noded triangular elements. The calculated SRF was 2.17, which is slightly lower than the value of 2.28 obtained from Bounds with no fractures in the slope. The difference here is not surprising given that, as discussed earlier, strength reduction analysis via FEM can lead to erroneous results on account of the inability to model post-failure behaviour.

Next, an analysis was performed which included the known fractures only, with the resulting DFN shown in Figure 5a. The lengths of the individual known fractures were not able to be randomly generated in RS2, and so the fracture extents were nominally set to half the distance between the points at which they were observed and their potential exit points on the slope outline. A mesh of approximately 10 000 elements was again generated, and a strength reduction analysis performed. Based on this, RS2 determined that the slope was unstable, with an SRF of 0.65 and apparent failure occurring along fracture 10, with large displacements calculated in the slope material above this fracture as indicated by the red/orange contours in Figure 5a. Analysis with Bounds based on the same fractures leads to a similar failure mechanism along the length of fracture 10 (Figure 5b), but with the slope stable at an SRF of 1.59, which is nearly 2.5 times higher than the value determined by RS2.

The reason why there is such a big difference between the SRF values determined by Bounds and RS2 comes back to the fact that, when carrying out strength reduction analysis via FEM, failure is defined as any state where convergence upon a solution for the load-displacement relations cannot be achieved (Hammah et al. 2004). In a fractured rock slope, significant deformation may occur due to slippage along the length of fractures without any rock actually breaking away from the slope, and this is what appears to be happening in the case of fracture 10 in

Figure 5. When using FELA, displacements are not computed and the SRF will always correspond to a state of collapse which, if not entirely governed by pre-existing fractures, will involve yielding of the rock mass material itself. In this way, FELA is more reliable at predicting collapse under general loading conditions when compared with FEM. Another advantage of using FELA is that strength reduction analysis can be performed much faster, as it is not necessary to trace the entire load-displacement path to failure as it is with FEM. Strength reduction analysis of the single DFN in Figure 5a took about 10 minutes with RS2, while one Monte Carlo simulation with Bounds typically took only 35 seconds for a similar sized mesh. Running 1000 Monte Carlo simulations with RS2, and manually changing the DFN in between each of them would be very time consuming.

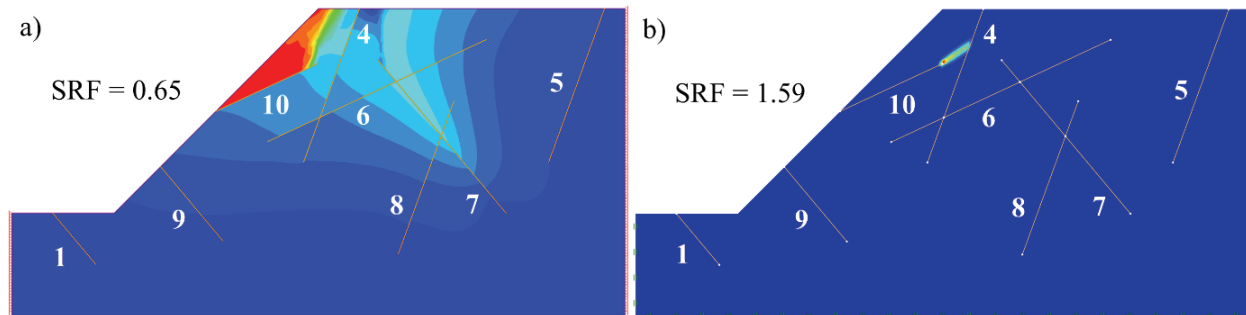


Figure 5. Plots of a) relative total displacement obtained from RS2 and b) relative shear dissipation obtained from Bounds for the 45 degree slope with known fractures

4 Conclusions

The method of strength reduction FELA has been successfully applied in the stability analysis of rock slopes with stochastic fractures. A new fracture generation algorithm which improves upon earlier developments by Andersson et al. (1984) has made for a practical means of generating DFNs based on fractures observed during field investigation. The implementation of the algorithm into the FELA program Bounds, together with its ability to be called automatically in Monte Carlo simulations of different DFNs, has made for a very efficient and robust means of determining a PoF that takes account of uncertainties associated with unknown fracture geometry. Strength reduction FELA was shown to be superior in terms of required run time, user intervention and ability to detect collapse when compared with the offerings of a commercial FEM package commonly used for stability analysis of rock slopes.

Acknowledgements

The authors are thankful for financial support received from the University of Newcastle and the Australian Research Council (DP200103390, DP220103381) whilst undertaking the research reported in this paper.

References

- Andersson, J., Shapiro, A.M. and Bear, J., 1984. A stochastic model of fractured rock conditioned by measured information. *Water Resources Research*, 20(1): 79-88.
- Brinkgreve, R.B.J. and Bakker, H.L., 1991. Non-linear finite element analysis of safety factors. *Proceedings of the 7th International Conference on Computer Methods and Advances in Geomechanics, Cairns (Australia)*. Rotterdam, A.A. Balkema, 1117-1122.
- Dyson, A.P. and Tolooiyan, A., 2018. Optimisation of strength reduction finite element method codes for slope stability analysis. *Innovative Infrastructure Solutions*, 3: 38.
- Hammah, R.E., Curran, J.H., Yacoub, T. and Corkum, B., 2004. Stability analysis of rock slopes using the finite element method. *Proceedings of the ISRM Symposium Eurock 2004 and 53rd Geomechanics Colloquium, Salzburg (Austria)*.
- Hoek, E. and Bray, J.W., 1981. *Rock Slope Engineering*. 3rd Edition, London, Taylor and Francis.
- Krabbenhöft, K. and Lyamin, A.V., 2015. Strength reduction finite-element limit analysis. *Géotechnique Letters*, 5: 250-253.
- Lyamin, A.V., Krabbenhöft, K. and Sloan, S.W., 2013. Adaptive limit analysis using deviatoric fields. *Proceedings of the 6th International Conference on Adaptive Modelling and Simulation, Lisbon, Barcelona, International Centre for Numerical Methods in Engineering (CIMNE)*, 448-455.
- Podlich, N.C., 2017. The Development of Efficient Algorithms for Large-Scale Finite Element Limit Analysis. *PhD Thesis, University of Newcastle*.
- Sloan, S.W., 2013. Geotechnical stability analysis. *Géotechnique*, 63(7): 531-572.
- Wolf Optimization, 2021. User Manual – Conic Optimization Solver v0.01a. Retrieved 11/10/2021 from https://www.wolfoptimization.com/public/Wolf_user_manual.pdf.